

# Supporting Information for “The regional hydroclimate response to stratospheric sulfate geoengineering and the role of stratospheric heating”

I. R. Simpson<sup>1</sup>, S. Tilmes<sup>1,2</sup>, J. H. Richter<sup>1</sup>, B. Kravitz<sup>3,4</sup>, D. G.

MacMartin<sup>5,6</sup>, M. J. Mills<sup>2</sup>, J. T. Fasullo<sup>1</sup>, A. G. Pendergrass<sup>1</sup>

<sup>1</sup>Climate and Global Dynamics Laboratory, National Center for Atmospheric Research, Boulder, CO, USA

<sup>2</sup>Atmospheric Chemistry Observations and Modelling Laboratory, National Center for Atmospheric Research, Boulder, CO, USA

<sup>3</sup>Department of Earth and Atmospheric Sciences, Indiana University, Bloomington, IN, USA

<sup>4</sup>Atmospheric Sciences and Global Change Division, Pacific Northwest National Laboratory, Richland WA, USA

<sup>5</sup>Mechanical and Aerospace Engineering, Cornell University, Ithaca, NY, USA

<sup>6</sup>Department of Computing and Mathematical Sciences, California Institute of Technology, Pasadena, CA, USA

## Contents of this file

1. Text S1
2. Table S1
3. Figures S1 to S5

### Text S1: Moisture budget analysis

Figures S6 and S7 present an analysis of the vertically integrated moisture budget for South America during JJA and the Mediterranean during DJF, following the methodology

---

outlined in Seager and Henderson (2013). The vertically integrated balance of moisture can be written

$$P - E = -\frac{1}{g\rho_w} \int_0^{p_s} (\bar{q}\nabla\cdot\vec{u}) - \frac{1}{g\rho_w} \int_0^{p_s} (\vec{u}\cdot\nabla\bar{q}) dp - \frac{1}{g\rho_w} \overline{q_s\vec{u}_s\cdot\nabla p_s} - \nabla\cdot \int_0^{p_s} \vec{u}'q' dp, \quad (1)$$

where it has been assumed that the time rate of change of moisture is negligible. Here  $\overline{(\cdot)}$  = monthly average,  $(\cdot)'$ =deviations from the monthly average,  $P$ =precipitation,  $E$ =evaporation,  $g$ =gravitational constant,  $\rho_w$ =density of water,  $t$ =time,  $q$ =specific humidity,  $p$ =pressure,  $\vec{u}$ =vector wind and  $(\cdot)_s$  denotes surface values. This budget has been calculated using 6 hourly instantaneous pressure level fields for a subset of BASE and GLENS members (5 members of each).

The balance (1) represents a decomposition into, from left to right on the right hand side, convergence of moisture associated with mass convergence of the stationary flow, convergence of moisture associated with advection across moisture gradients by the stationary flow, a surface term associated with surface flow up and down pressure gradients (can be thought of as representing orographic precipitation and includes both stationary and transient components) and the convergence of moisture associated with sub-monthly transient fluxes. The combination of the first and second terms on the right will be referred to as the “stationary contribution”, the third term will be referred to as the “surface term” and the fourth will be referred to as the “transient contribution”.

The extent to which this budget closes can be assessed by comparison of the “P-E” panel with the “Sum” panel in each figure. The budget closure is comparable to those in other studies (Seager & Henderson, 2013; Seager et al., 2014) with only small residuals that exist primarily over land regions with topography where inaccuracies due to the

intersection of pressure levels with topography or the inconsistency, compared to model numerics, in the calculation of divergence, become important.

Over many of the regions discussed in the main text, this budget is not particularly useful as the dominant term is the first on the right hand side i.e., changes in  $P - E$  are balanced by anomalous mass convergence by the stationary flow. Since mass convergence and precipitation are strongly connected, this does not provide much information as to the underlying cause of the hydroclimate changes.

It is, however, worthwhile to consider this balance over Patagonia during JJA and the Mediterranean during DJF to assess the contribution played by anomalous transient moisture flux convergence in these regions. In these regions and seasons, the precipitation response to stratospheric heating was found to be very similar to the full GLENS response. This is despite the fact that the transient eddy activity weakens considerably more in GLENS than in the stratospheric heating experiments (Figs 4 and 5 e and f of the main text).

For South America during JJA, the reason for this can be understood from Fig. S6. Over the southern tip of South America, even though the transient eddy activity weakens in GLENS, the change in transient moisture flux convergence does not play an important role in the altered moisture budget (Fig. S6k). Instead, it is the surface term that is dominating to give rise to the drying on the west coast of the Southern portion of Chile. This is presumably a reduction in orographic precipitation associated with the reduced zonal flow impinging on the Andes in this region. This reduced zonal flow occurs in both GLENS and the stratospheric heating experiments (Figs. 4 and 5 b and c of the main text) and so it makes sense that the precipitation changes in GLENS and the stratospheric

heating experiments should be so similar despite the greater weakening in transient eddy activity in GLENS compared to GEOHEAT.

Similar conclusions can be drawn for the Mediterranean during DJF (Fig. S7). The drying in Southern Europe and wetting to the North can primarily be attributed to altered stationary moisture flux convergence (Fig. S7l), in particular the advective component of that (Fig. S7p) which largely arises from advection in the zonal direction (Fig. S7q). The changes in the zonal flow are similar between GLENS and GEOHEAT so it makes sense that both exhibit a drying over southern Europe and a wetting to the North. Climatologically, the transients act to moisten much of Europe and western Russia. In line with the weakened transient eddy activity over Europe in GLENS (Fig 5e of the main text), there is a reduced convergence of moisture over much of central Europe and Western Russia by the transients (Fig. S7m). Since the transient eddy activity does not reduce as much in the stratospheric heating experiments, they do not exhibit as much of a drying over central Europe as in GLENS and they exhibit more of a wetting over Scandinavia and western Russia (compare Figs 14 d and e of the main text). So, the similarity in the pattern of reduced precipitation over the Mediterranean countries and increased precipitation over Scandinavia and Western Russia between GLENS and GEOHEAT/GEOHEAT\_S can be understood given the importance of the altered zonal advection in contributing to this response. But the greater weakening of transient eddy activity and the associated reduced moisture flux convergence over central Europe in GLENS results in a slightly different pattern of change in that region.

## References

Schneider, U., Becker, A., Finger, P., Meyer-Christoffer, A., & Ziese, M. (2018). *GPCC*



:  
*Full Data Monthly Product Version 2018 at 0.5°: Monthly Land-Surface Precipitation from Rain-Gauges built on GTS-based and Historical Data.* DWD. Retrieved from [http://dx.doi.org/10.5676/DWD\\_GPCC/FD\\_M\\_V2018\\_050](http://dx.doi.org/10.5676/DWD_GPCC/FD_M_V2018_050) doi: 10.5676/DWD\_GPCC/FD\_M\_V2018\_050

Seager, R., & Henderson, N. (2013). Diagnostic Computation of Moisture Budgets in the ERA-Interim Reanalysis with Reference to Analysis of CMIP-Archived Atmospheric Model Data. *J. Clim.*, *26*, 7876–7901.

Seager, R., Liu, H., Henderson, N., Simpson, I., Kelley, C., Shaw, T., . . . Ting, M. (2014). Causes of Increasing Aridification of the Mediterranean Region in Response to Rising Greenhouse Gases. *J. Clim.*, *27*, 4655–4676.

**Table S1.** List of CMIP5 models and number of members of RCP8.5 simulation used

Model	#members
ACCESS1-0	1
ACCESS1-3	1
bcc-csm1-1	1
bcc-csm1-1-m	1
BNU-ESM	1
CanESM2	5
CCSM4	6
CESM1-CAM5	3
CESM1-WACCM	3
CMCC-CM	1
CMCC-CMS	1
CNRM-CM5	5
CSIRO-Mk3-6-0	10
FGOALS-g2	1
FIO-ESM	3
EC-EARTH	2
GFDL-CM3	1
GFDL-ESM2G	1
GFDL-ESM2M	1
GISS-E2-H	2
GISS-E2-R	2
HadGEM2-AO	1
HadGEM2-CC	3
HadGEM2-ES	4
inmcm4	1
IPSL-CM5A-LR	4
IPSL-CM5A-MR	1
IPSL-CM5B-LR	1
MIROC5	3
MIROC-ESM	1
MIROC-ESM-CHEM	1
MPI-ESM-LR	3
MPI-ESM-MR	1
MRI-CGCM3	1
NorESM1-M	1
NorESM1-ME	1

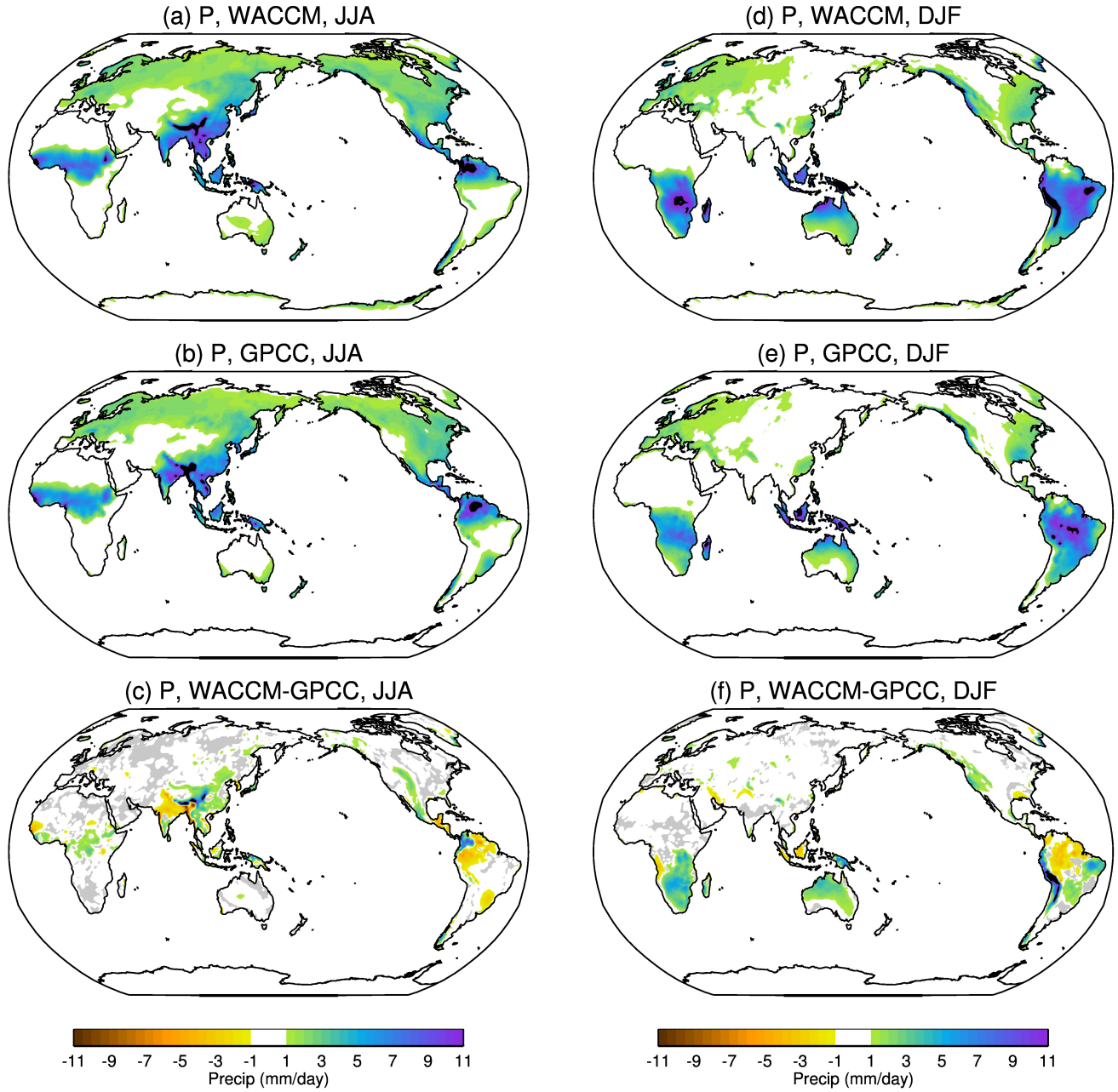


**Figure S1.** Precipitation climatologies from 1980-2016 over land for (left) DJF and (right) JJA. (Top) CESM-WACCM, (middle) GPCC (Schneider et al., 2018) and (bottom) CESM-WACCM - GPCC. Gray shading in (c) and (f) shows regions where the difference between CESM-WACCM and GPCC is not statistically significant from zero at the 95% level by a one-sided t-test assuming each year between 1980 and 2016 is independent.

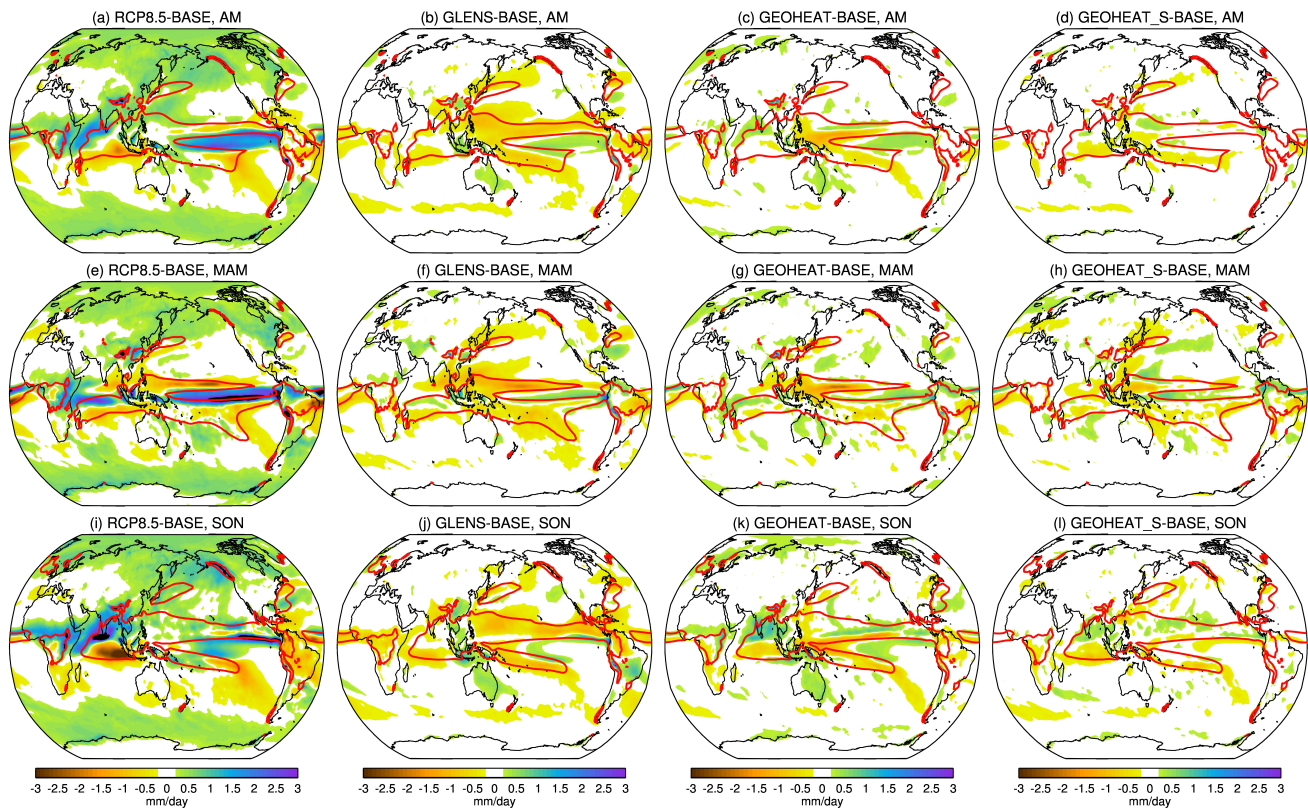


**Figure S2.** Precipitation anomalies (left column) RCP8.5-BASE, (2nd column) GLENS-BASE, (3rd column) GEOHEAT-BASE and (right column) GEOHEAT\_S-BASE. (top) Annual mean, (2nd row) March-April-May (MAM), (bottom) September-October-November (SON). Red contour shows the 5mm/day contour of the BASE climatology.

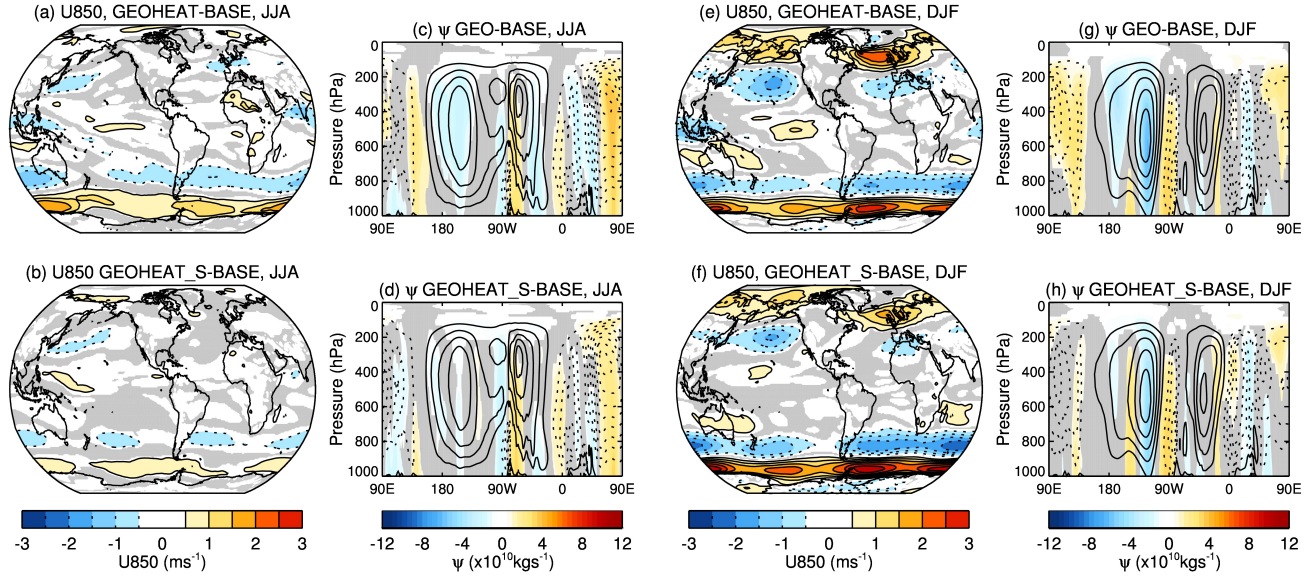


**Figure S3.** A comparison of the 850hPa zonal wind and zonal streamfunction responses between GEOHEAT and GEOHEAT\_S. (a)/(b) shows JJA 850hPa zonal wind for GEOHEAT-BASE/GEOHEAT\_S-BASE and (c)/(d) show JJA zonal streamfunction averaged over 5°S to 5°N for GEOHEAT-BASE and GEOHEAT\_S-BASE. (g)-(h) are as (a)-(d) but for DJF. Gray shading indicates regions where the difference is not significantly different from zero at the 95% level by a one sided test using the bootstrapping methodology outlined in section 2.2 of the main text.



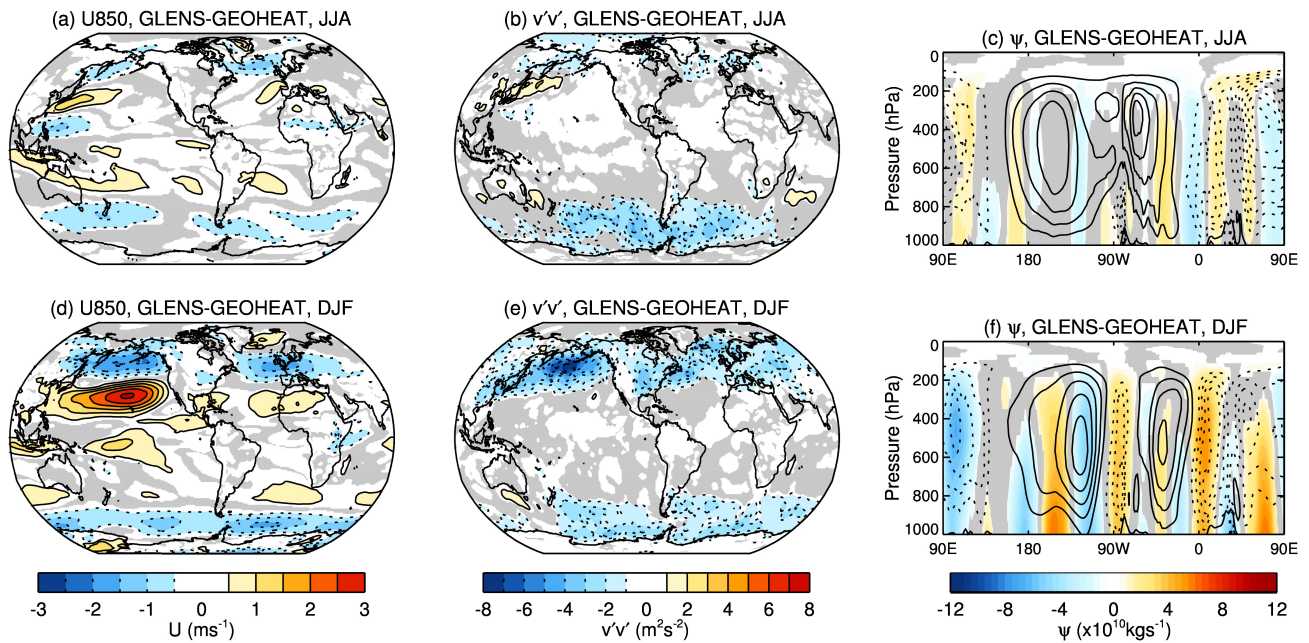


**Figure S4.** (a)-(c) JJA and (d)-(f) DJF differences between GLENS and GEOHEAT. (a)/(c) 850hPa zonal wind, (b)/(e) 850hPa 10 day high pass filtered eddy meridional wind variance ( $v'v'$ ) and (c)/(f) zonal stream function averaged over  $5^{\circ}\text{S}$  to  $5^{\circ}\text{N}$ . Grey shading shows regions where GEOHEAT is not significantly different from GLENS at the 95% level by a one sided test using the bootstrapping methodology outlined in section 2.2 of the main text.

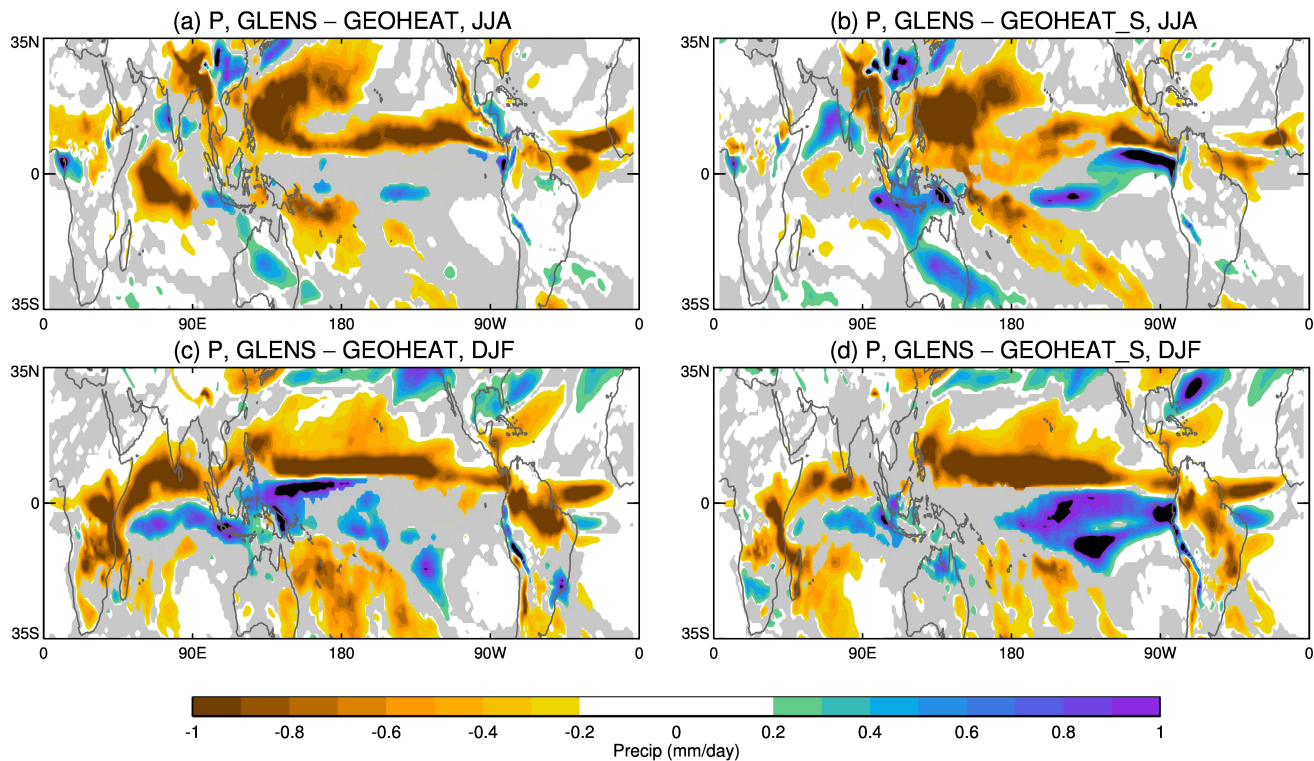


**Figure S5.** (a) difference in precipitation between GLENS and GEOHEAT during JJA with gray shading showing regions where GLENS and GEOHEAT are not significantly different from each other at the 95% level. Significance is calculated via the bootstrapping method described in section 2.2 but instead of bootstrapping from BASE, the bootstrapping is performed on GLENS. (b) as (a) but for the difference between GLENS and GEOHEAT\_S. (c) and (d) are as (a) and (b) but for the DJF season.

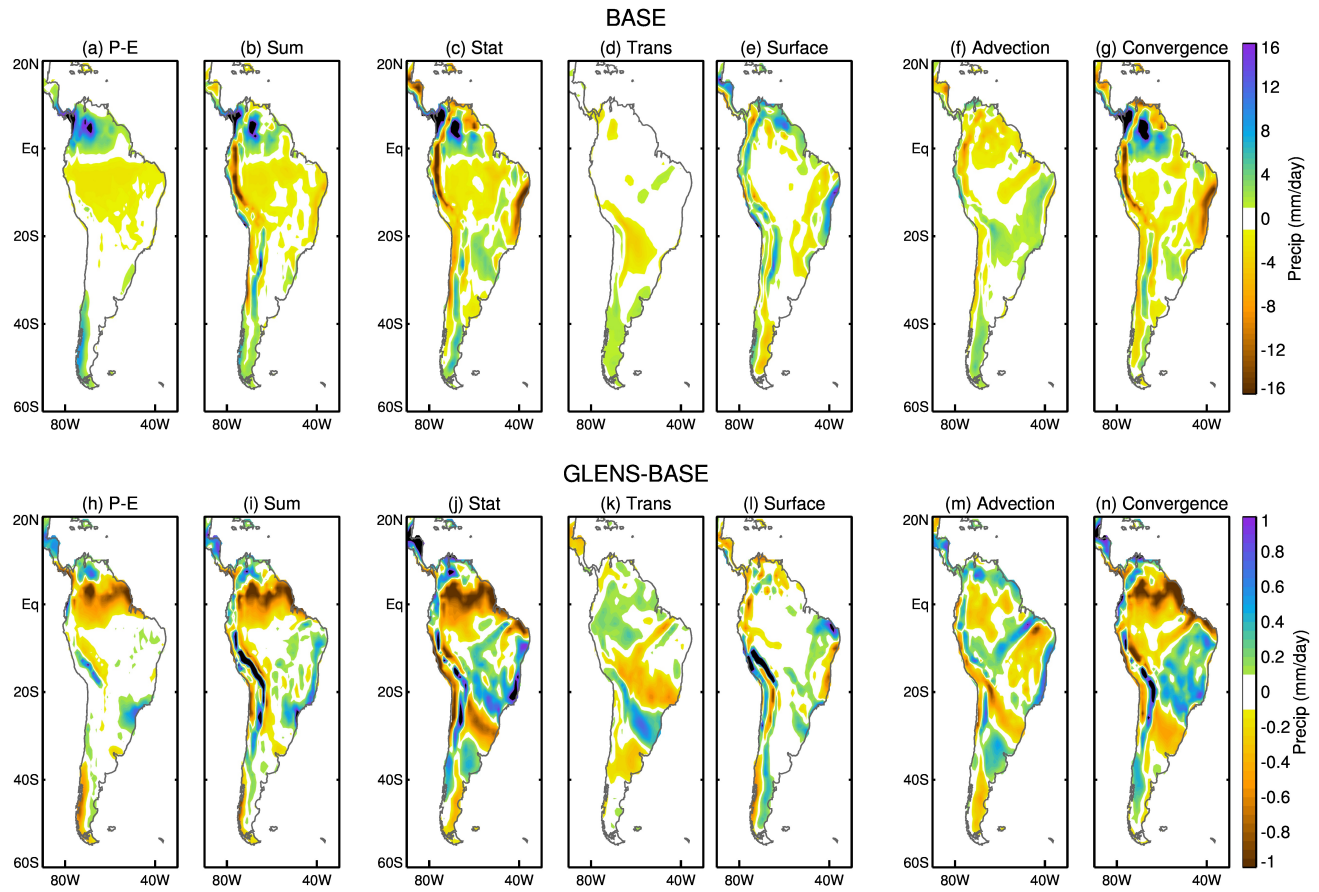


**Figure S6.** JJA moisture budget over South America for (Top) BASE and (bottom) GLENS-BASE. From left to right: P-E, Sum of terms in (1), the stationary contribution, the transient contribution, the surface contribution, the component of the stationary contribution due to horizontal advection and the component of the stationary contribution due to mass convergence.



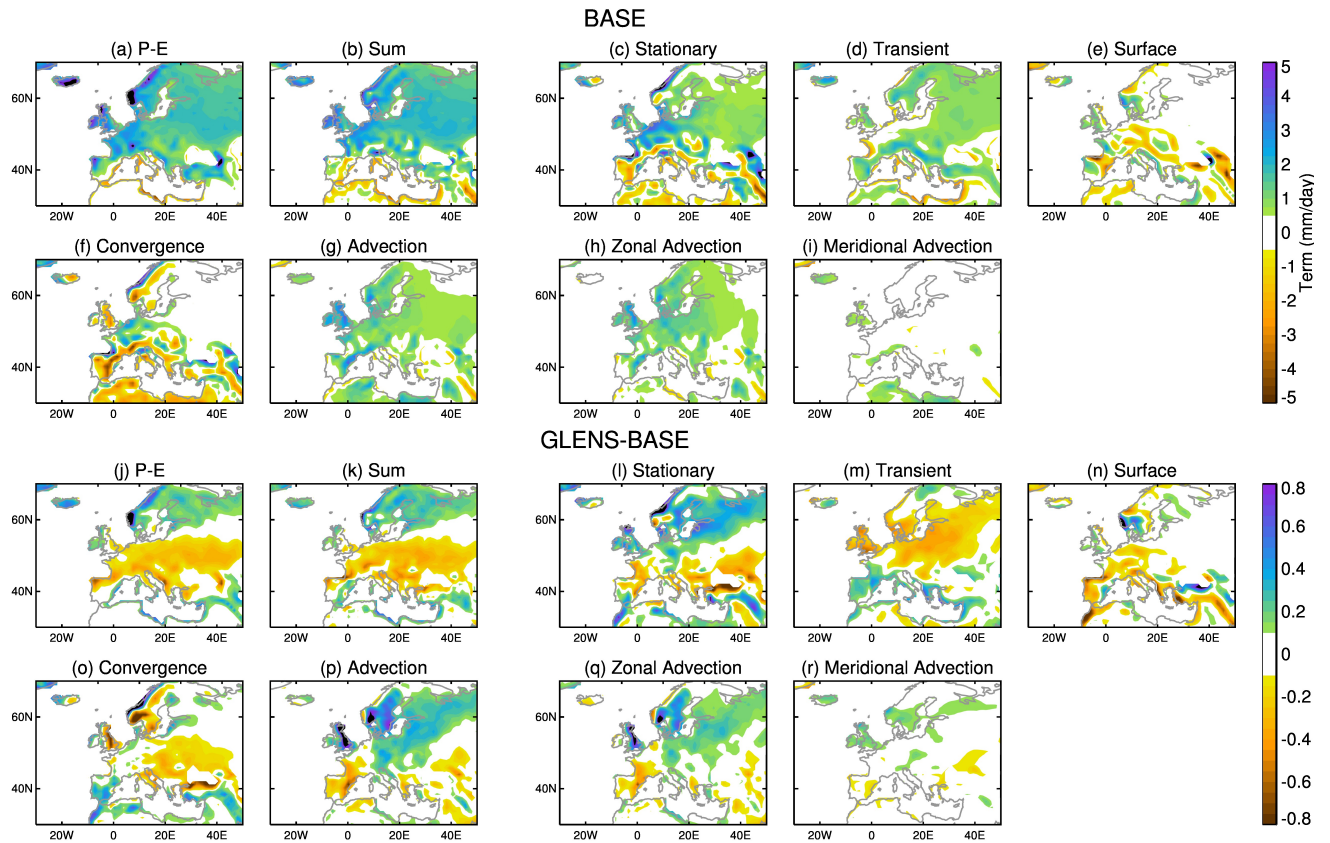


**Figure S7.** DJF moisture budget over the Mediterranean and Europe. (a)-(i) show BASE budget terms. (a) P-E, (b) the Sum of budget terms and (c)-(e) the stationary, transient and surface contributions. In (f) and (g) the stationary contribution has been divided up in the mass convergence and advection components and in (h) and (i) the advection contribution has been divided up into zonal advection and meridional advection. (j)-(r) are as (a)-(i) but for GLENS-BASE.